Supporting information for

Multicolor STED Imaging of Cells and Extracellular Vesicles using Xanthene-conjugated Polymer Dots

Peixiang Li[†b,c] , Kehua Tang[†a,c], Yachen Ying[†c],Long Chen[c],Qin Shentu[c] ,Yating Xiao[c], Lubin Qi[c,d],Ren Cai[f], Qiongzheng Hu[e],Jiantao Ping*[e] ,Xiaohong Fang*[a,c,d]and Yifei Jiang*[a,b,c,d]

[a.] *School of Materials Science and Engineering, Tianjin University, Tianjin 300350 China.*
[b.] *Zhejiang University of Technology, Hangzhou 310014, P. R. China.*
[c] *Hangzhou Institute of Medicine (HIM), Chinese Academy of Sciences, Hangzhou, Zhejiang 310022, P. R China.*
[d.] *ZheJiang Cancer Hospital Hangzhou, Zhejiang 310022, P. R. China.*
[e.] *Shandong Analysis and Test Center, Qilu University of Technology (Shandong Academy of Sciences), Jinan 250014,P.R China.*
[f.] *College of Material Science and Engineering, Hunan University, Changsha, Hunan 410082,China.*

The corresponding authors:
Yifei Jiang
jiangyf@ibmc.ac.cn
Xiaohong Fang
xfang@iccas.ac.cn
Jiantao Ping
pingjt@qlu.edu.cn

Contents

1. Experimental Section

1.1. Synthesis of PL-OH

A 50 mL round-bottom flask was charged with 4-chloromethylstyrene (1.0 g, 6.58 mmol), ethylene glycol (11.0 g, 17.7 mmol), and 3 mL of a 1 M aqueous NaOH solution. The reaction mixture was stirred at 70 °C for 6 hours. Upon completion, the crude product was concentrated under reduced pressure and subsequently purified via silica gel column chromatography, employing a petroleum ether/ethyl acetate mixture (100:45, v/v) as the eluent, yielding PS-OH as a colorless oil (866 mg).

^{1}H NMR (400 MHz, Acetonitrile-d3) δ 7.29 -7.02 (m, 4H), 6.54 (dd, J = 17.6, 10.9 Hz, 1H), 5.58 (dd, J = 17.6, 0.9 Hz, 1H), 5.08 (dd, J = 10.9, 0.8 Hz, 1H), 4.33 (s, 2H), 3.54 (dd, J = 9.6, 5.3 Hz, 2H), 3.43 – 3.33 (m, 2H), 3.29 (t, J = 5.8 Hz, 1H).

PS-OH (400 mg, 2.25 mmol) and styrene (2.35 g, 22.60 mmol) were dissolved in toluene (10 mL) and subjected to thorough stirring in a reaction flask. Under an inert nitrogen atmosphere, 2,2′-azobis(2-methylpropionitrile) (AIBN, 5 mg, 0.03 mmol) was introduced, and the reaction mixture was maintained at 70 °C with continuous stirring for 12 hours. Upon completion of the reaction, the solution was concentrated under reduced pressure and subsequently added dropwise into hexane (100 mL) under stirring conditions to facilitate polymer precipitation. The resulting precipitate was collected via filtration, dissolved in dichloromethane (DCM), and subjected to two cycles of reprecipitation in methanol. The final product was dried under vacuum at 80 °C for 12 hours, yielding PL-OH as a white solid (1.32 g).

1.2. Synthesis of Xanthene 640

1.2.1. Synthesis of Compound 1

4-Bromo-3-methylbenzoic acid (1.50 g, 7.0 mmol) and oxalyl chloride (0.90 mL, 10.5 mmol) were dissolved in anhydrous dichloromethane (DCM, 20 mL). A catalytic amount of anhydrous N, N-dimethylformamide (DMF, 4–5 drops) was added dropwise via syringe under a nitrogen atmosphere. The reaction mixture was stirred at ambient temperature for 4 h (see scheme in the first panel of Fig. S4). Upon completion, the solvent was removed under reduced pressure to afford the crude acyl chloride intermediate, which was used directly in the subsequent step without further purification due to its high sensitivity toward moisture.

The residue was dissolved in anhydrous tetrahydrofuran (THF, 35 mL) and cooled to 0 °C under a nitrogen atmosphere. A solution of potassium tert-butoxide (1.57 g, 14.0 mmol) in anhydrous THF (21 mL) was then added slowly to the reaction mixture. After completion of the addition, the ice bath was removed, and the reaction mixture was allowed to warm to ambient temperature and stirred for an additional 3 h (see scheme in the first panel of Fig. S4). The solvent was then removed under reduced pressure, and the residue was dissolved in ethyl acetate (AcOEt). The organic phase was washed successively with water and brine, dried over anhydrous sodium sulfate (Na_2SO_4), filtered, and concentrated. The resulting residue was purified by silica gel column chromatography to afford compound 1 as a yellow oil (0.75 g, 40%).

^{1}H NMR (400 MHz, $CDCl_3$) δ 7.83 (s, 1H), 7.64 (dd, *J* = 8.3, 2.5 Hz, 1H), 7.56 (d, *J* = 8.3 Hz, 1H), 2.43 (s, 3H), 1.58 (s, 9H).

1.2.2. Synthesis of Compound 2

Compound 1 (1.00 g, 3.70 mmol) was dissolved in anhydrous tetrahydrofuran (THF, 30 mL) and subsequently cooled to −78 °C. Under an inert nitrogen atmosphere, a 1.6 M solution of n-butyllithium (n-BuLi) in n-pentane (0.11 mL, 177 µmol) was added to the reaction mixture in a slow, dropwise manner while maintaining the temperature at −78 °C. The mixture was stirred under these conditions for 1 hour. Following this, a solution of 3,7-bis(dimethylamino)-5,5-dimethyldibenzo[b,e]silin-10(5H)-one (300 mg, 0.93 mmol) in anhydrous THF (20 mL) was introduced dropwise using a syringe, also at −78 °C (see scheme in the second panel of Fig. S4). Upon completion of the addition, the reaction mixture was allowed to gradually reach room temperature and was stirred for an additional 3 hours.

The reaction was terminated by the addition of 0.1 M hydrochloric acid in aqueous solution, subsequently neutralized with a saturated aqueous solution of sodium bicarbonate. The resulting mixture was then subjected to extraction using dichloromethane (DCM). The combined organic phases were washed with a brine solution, dried over anhydrous sodium sulfate, filtered, and concentrated to yield a blue solid (compound 2). This compound was utilized directly in the subsequent step without additional purification.

Compound 2 was dissolved in a solvent system comprising 6 M aqueous hydrochloric acid (60 mL)

and acetonitrile (20 mL), followed by stirring at 40 °C for a duration of 2 hours. Upon cooling to ambient temperature, the pH of the reaction mixture was adjusted to a range of 2–3 through the addition of 2 M aqueous sodium hydroxide. The mixture was subsequently subjected to extraction using dichloromethane (DCM). The combined organic layers were washed with a brine solution, dried over anhydrous sodium sulfate (Na_2SO_4), filtered, and concentrated. The resultant residue underwent purification via silica gel column chromatography, yielding compound 3 as a blue solid（12mg）.

1.3. Synthesis of Xanthene -grafted polymer

Under a nitrogen atmosphere, Xanthene 488 (50 mg) and polymer PL-OH were dissolved in dichloromethane (DCM, 15 mL) and stirred at 0 °C. Subsequently, 1-(3-dimethylaminopropyl)-3-ethylcarbodiimide hydrochloride (EDC, 100 mg, 0.52 mmol) and 4-dimethylaminopyridine (DMAP, 10 mg, 0.08 mmol) were added. The reaction mixture was gradually warmed to room temperature and stirred for 6 h. After completion, the reaction mixture was concentrated under reduced pressure to 1–2 mL and added dropwise into methanol (200 mL) under stirring. The resulting precipitate was collected and reprecipitated twice to afford PL-Xanthene 488 (80 mg). By replacing Xanthene 488 with Xanthene 561 or Xanthene 640 and following identical synthetic procedures, PL-Xanthene 561 and PL-Xanthene 640 were successfully prepared, respectively.

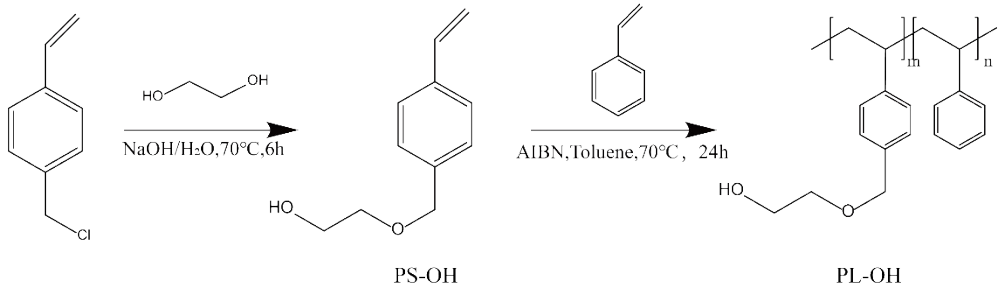

Figure S1. Synthesis of PL-OH

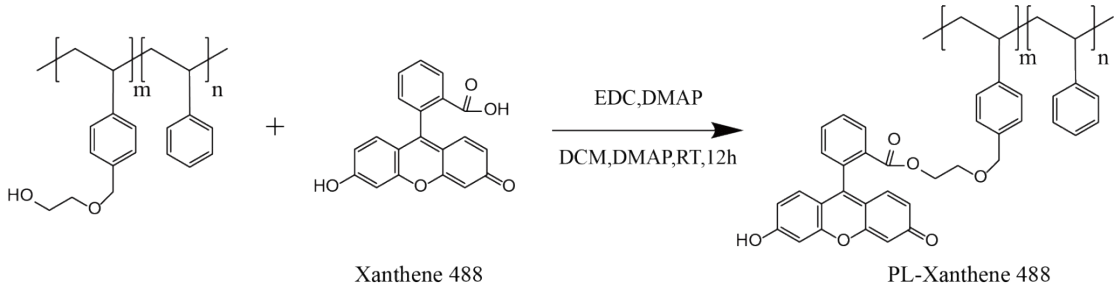

Figure S2. Covalent grafting of Xanthene 488 onto polystyrene backbones.

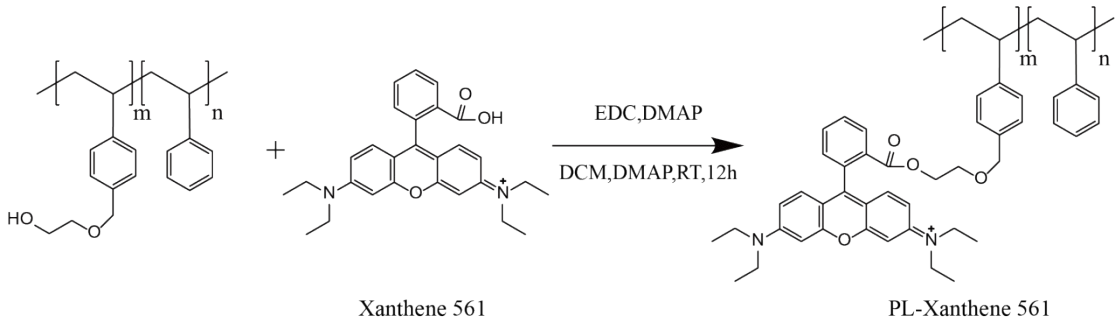

Figure S3. Covalent grafting of Xanthene 561 onto polystyrene backbones.

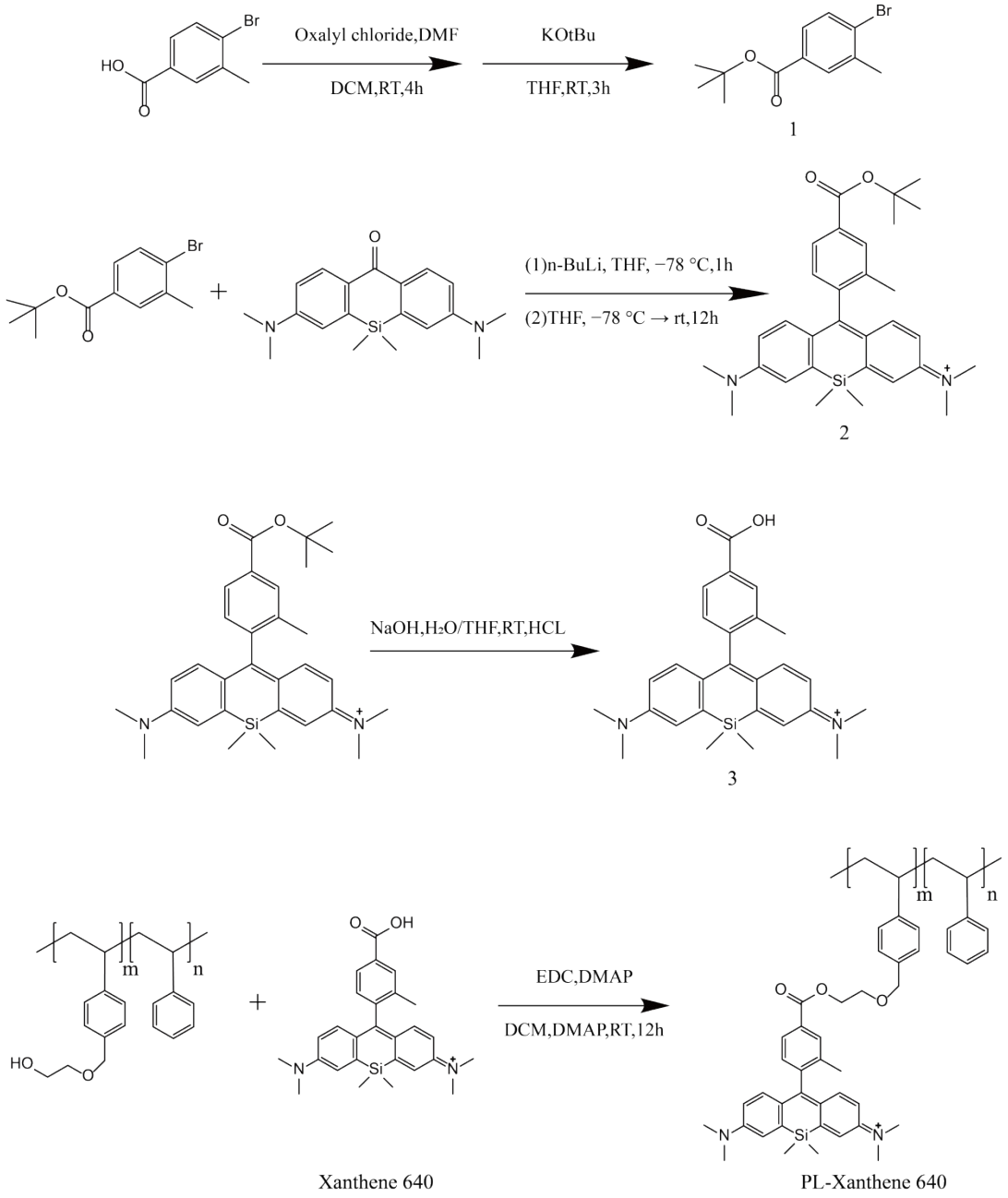

Figure S4. Synthesis of Xanthene and Covalent grafting of Xanthene 640 onto polystyrene backbones.

1.4. Preparation of Single-particle Imaging Sample

Clean glass coverslips were immersed in a saturated solution of sodium hydroxide and isopropanol for 30 minutes, followed by ultrasonication in deionized water for an additional 30 minutes, and subsequently rinsed thoroughly with deionized water. The cleaned coverslips were then dried under a stream of nitrogen. An ethanolic solution of (3-aminopropyl) triethoxysilane (APTES) at a concentration of 0.0005 M was prepared, and 80 µL of this solution was uniformly

drop-cast onto the surface of the coverslips. After allowing the solution to stand for approximately 5 minutes, the coverslips were rinsed three times with deionized water and dried under a nitrogen stream.

The aqueous dispersion of Pdots was diluted to a concentration of 1–2 ppm. A volume of 200 µL of this diluted solution was applied to an aminated coverslip and incubated for a duration of 30–40 minutes. Following incubation, the coverslip underwent three rinses with deionized water to eliminate any unbound nanoparticles and was subsequently dried using a nitrogen stream. The prepared coverslips were then stored in 50 mL centrifuge tubes filled with nitrogen until further use.

1.5. Bioconjugation.

The bioconjugation of xPdots was accomplished through an EDC-mediated coupling reaction between the carboxyl groups on the surface of the xPdots and the amino groups of biomolecules, facilitating the synthesis of xPdots conjugated with streptavidin (SA) or immunoglobulin G (IgG).

As a representative example, SA-conjugated xPdots were synthesized by initially combining 4 mL of xPdots aqueous dispersion with 80 µL of polyethylene glycol (PEG, 5 wt%). This was followed by the sequential incorporation of 80 µL of DNA-grade HEPES buffer (1 M) and 30 µL of streptavidin solution (11.5 mg mL^{-1}), with thorough vortexing after each addition. Subsequently, 40 µL of freshly prepared 1-ethyl-3-(3-dimethylaminopropyl) carbodiimide hydrochloride (EDC, 5 mg mL^{-1}) was introduced, and the reaction mixture was allowed to proceed on a shaker at ambient temperature for a duration of 4 hours.

To inhibit nonspecific binding, 80 µL of bovine serum albumin (BSA, 10% w/v) was added, followed by incubation on a shaker for an additional 30 minutes. Subsequently, the reaction mixture underwent purification using ultrafiltration tubes: a 100 kDa molecular weight cutoff (MWCO) tube was employed for xPdots–SA conjugates, while a 300 kDa MWCO tube was utilized for xPdots–IgG conjugates. During the purification process, five cycles of buffer exchange were conducted using a washing buffer consisting of 0.1% (w/v) PEG, 2% (w/v) HEPES, and 97.9% (w/v) H_2O.

Purified xPdots conjugates were concentrated to 1 mL, stabilized with BSA (100 µL, 10% w/v), and stored at 4 °C in the dark. NaN_3 (10 µL, 300 mM) was added for long-term preservation. IgG–

xPdots were prepared analogously by replacing SA with IgG (12 μL, 5 mg mL^{-1}).

1.6. Multicolor STED imaging in cells

As an example of cellular microtubule (tubulin) labeling, BS-C-1 cells were seeded onto 8-well chambered slides at a density of approximately 3×10^4 cells per well and cultured for 18 h to allow sufficient adhesion. The cells were then sequentially subjected to permeabilization, fixation, and reduction, followed by washing three times with PBS.

The treated cells were incubated with a primary anti-β-tubulin antibody (200 μL, 5 μg mL^{-1}, rabbit monoclonal antibody against β-tubulin) for 1 h, followed by washing three times with PBS. Subsequently, a biotinylated goat anti-rabbit IgG secondary antibody (H&L) (200 μL, 5 μg mL^{-1}) was added and incubated for an additional 1 h, after which the cells were again washed three times with PBS.

SA-conjugated xPdots (200 μL; including xPdots 488, xPdots 561, and xPdots 640) were then introduced and incubated for 1 h to complete fluorescent labeling. After incubation, the samples were washed three times with PBS and stored at 4 °C prior to subsequent imaging experiments.

To systematically assess the targeting specificity of bioconjugated xPdots, three representative intracellular subcellular structures were selected as imaging targets. Specific labeling of three classes of cellular markers was accomplished through the use of streptavidin (SA) or immunoglobulin G (IgG) conjugation strategies. Specifically, xPdots 488 conjugated with SA were utilized for the recognition of microtubules (tubulin); xPdots 561 conjugated with goat anti-rabbit IgG (H&L) were employed to label LaminB1; and xPdots 640 conjugated with goat anti-mouse IgG were used to target clathrin. To evaluate the efficacy of xPdots in STED imaging of cellular microtubules, cells labeled with xPdots were imaged using both confocal fluorescence microscopy and STED super-resolution microscopy. The labeling quality and imaging performance were then systematically evaluated.

The laser power settings for the white-light lasers and STED depletion lasers on the Leica DMi8 microscope, using a 100× oil immersion objective, were as follows: For white-light lasers, at 100% excitation intensity, the measured powers were 25 μW at 488 nm, 33 μW at 561 nm, and 45 μW at 638 nm. For the STED depletion lasers, the powers corresponding to 5% depletion intensity were

17 mW at 592 nm, 11.26 mW at 660 nm, and 16.25 mW at 775 nm. The imaging parameters for each xPdots were as follows: xPdots 488: excitation at 488 nm (20% laser power), emission collected at 500-550 nm, STED depletion at 592 nm (60% laser power); xPdots 561: excitation at 561 nm (20% laser power), emission collected at 550-650 nm, STED depletion at 660 nm (80% laser power); xPdots 640: excitation at 640 nm (20% laser power), emission collected at 700-750 nm; STED depletion at 775 nm (40% laser power).

1.7. Multicolor STED imaging of EVs

Initially, a streptavidin (SA) solution at a concentration of 1 mg mL^{-1} was introduced into the microfluidic channels, which contained glass substrates that had been previously aminated and subsequently modified with Biotin-PEG-NHS and mPEG-NHS. The solution was incubated for 20 minutes to facilitate the immobilization of SA on the channel surfaces. Following this incubation period, the channels were washed three times with Dulbecco's Phosphate-Buffered Saline (DPBS) to eliminate any unbound SA.

For the biotinylation of extracellular EVs, a volume of 20 µL of EVs, at a concentration of 1×10^{10} mL^{-1}, was diluted in 200 µL of DPBS. Concurrently, 5 µL of Biotin-PEG-DSPE was diluted in 280 µL of DPBS. The two solutions were then thoroughly mixed by vortexing and incubated for 10 minutes to facilitate the incorporation of Biotin-PEG-DSPE into the EV membrane. Subsequently, the reaction mixture was purified using an agarose gel column to eliminate any unbound DSPE-PEG-Biotin. The purified EV solution was concentrated to a final volume of 100 µL using an ultrafiltration unit with a molecular weight cutoff (MWCO) of 100 kDa. The concentrated EV suspension was then introduced into microfluidic channels and incubated for 20 minutes to allow for EV capture, followed by three washes with DPBS to ensure removal of unbound components.

Following the immobilization of extracellular EVs, sequential immunolabeling was conducted. Initially, a rabbit anti-CD63 monoclonal antibody was prepared at a concentration of 1 µg/mL in DPBS and introduced into the microfluidic channels. This was incubated for 45 minutes, after which the channels were washed three times with DPBS. Subsequently, a mouse anti-CD9 monoclonal antibody, also diluted to a concentration of 1 µg/mL, was introduced into the channels and incubated for an additional 45 minutes, followed by three washes with DPBS.

Finally, xPdots 640 conjugated with goat anti-mouse IgG were introduced and incubated for 45 minutes, followed by three washes with DPBS. Subsequently, xPdots 561 conjugated with goat anti-rabbit IgG (H&L) were introduced and incubated for 45 minutes, followed by three washes with DPBS. Finally, SA-conjugated xPdots 488 were introduced, incubated for 45 minutes, and washed three times with DPBS. The prepared microfluidic chips were then stored at 4 °C until imaging experiments were conducted. The STED imaging was conducted with the same parameters as describe above.

2. Supplementary Figures and Discussions

2.1. Effect of different fluorophore ratios on Pdots

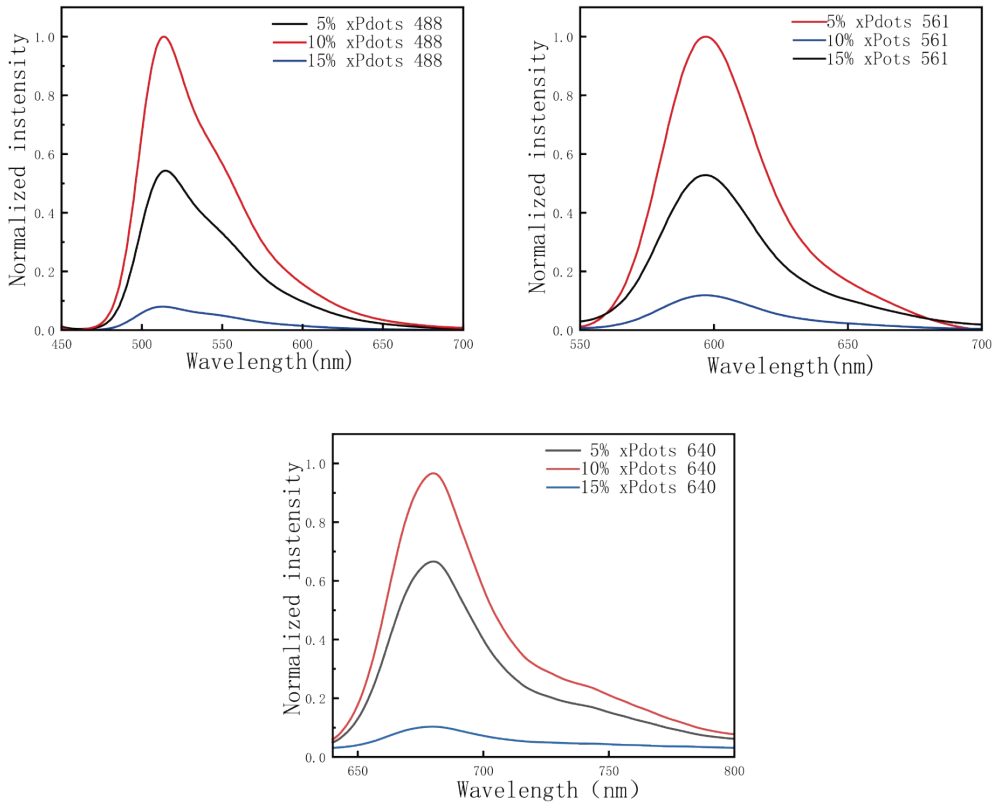

Figure S5. presents the normalized fluorescence emission spectra of xPdots 488, xPdots 561, and xPdots 640 prepared with different fluorophore loading ratios (5%, 10%, and 15%). For all three xPdots, the fluorescence emission intensity increased when the fluorophore ratio was increased from 5% to 10%. In contrast, a further increase of the fluorophore ratio to 15% led to a marked decrease in emission intensity. This non-monotonic dependence indicates that excessive fluorophore loading induces concentration-dependent quenching, thereby reducing the overall fluorescence output.

2.2. Physicochemical characterization of xPdots

Probe	Abs(nm)	FL(nm)	Size(nm)	ζ（mV）	Mn
xPdots 488	490	515	24	-27.6	29093
xPdots 561	561	595	21	-30.3	22920
xPdots 640	655	682	21	-26.8	26843

Table 1. summarizes the physicochemical properties of the three xPdots probes, including their absorption and emission maxima, hydrodynamic sizes, ζ-potentials, and number-average molecular weights (Mn).

As listed in the table, xPdots 488, xPdots 561, and xPdots 640 exhibit absorption peaks at 490, 561, and 655 nm and corresponding emission maxima at 515, 595, and 682 nm, respectively. All three xPdots show small hydrodynamic diameters in the range of 21–24 nm and negative ζ-potentials between −26.8 and −30.3 mV. These physicochemical characteristics indicate that the xPdots form uniformly sized nanoparticles and possess sufficient electrostatic repulsion, which is favorable for maintaining stable dispersion in aqueous solution. Together, these features suggest that the xPdots exhibit good colloidal stability under physiological conditions.

2.3. Photostability of xPdots compared with small-molecule dyes

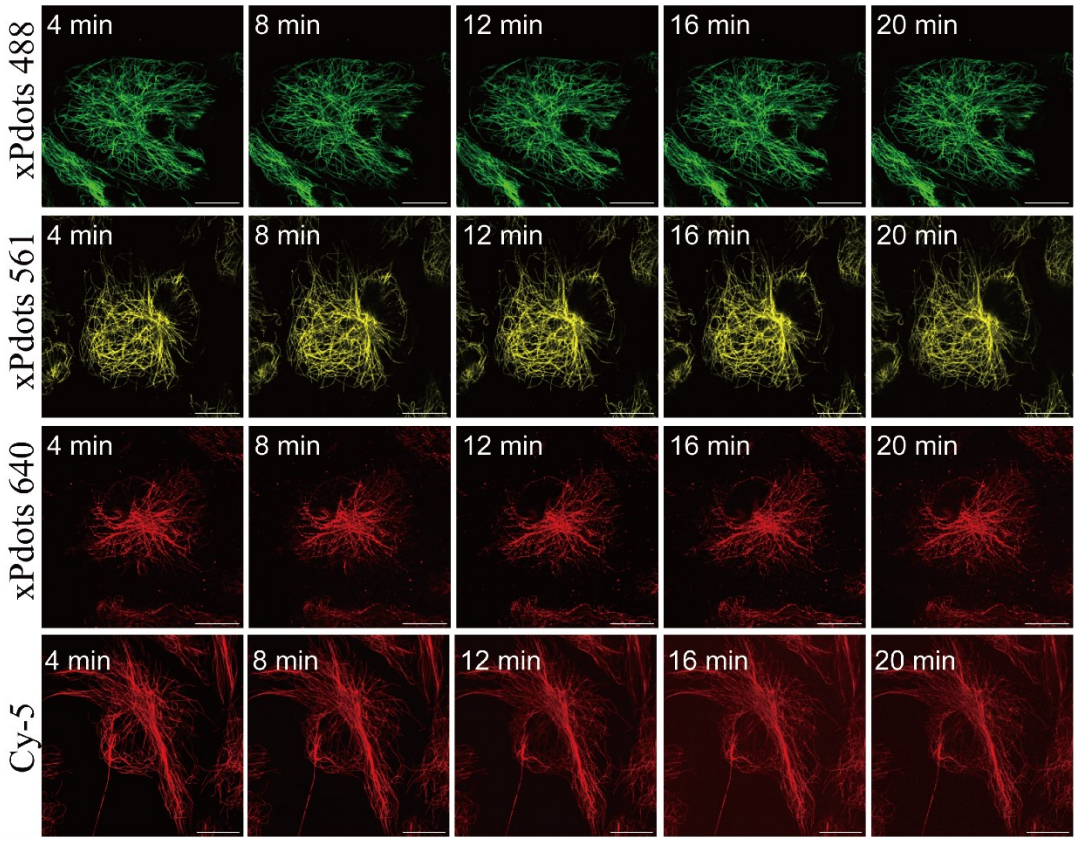

Figure S6. Photostability comparison of xPdots and Cy5 under continuous laser irradiation.

Time-lapse fluorescence images of cellular microtubules labeled with xPdots 488, xPdots 561, xPdots 640, and the small-molecule dye Cy5 acquired under continuous laser irradiation for 20 min. The images were obtained using a 95B camera at an exposure time of 200 ms and 10% corresponding excitation light intensity (30 mW) for three xPdots (488 nm/561 nm/638 nm) and Cy5 (638 nm).

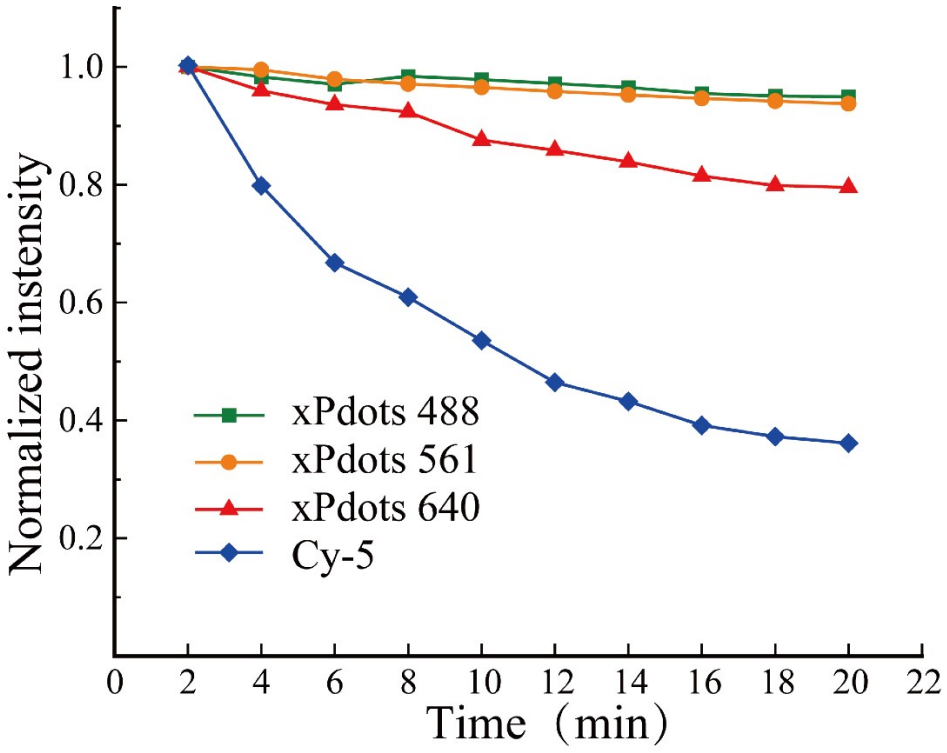

Figure S7. Quantitative analysis of photostability under continuous laser irradiation.

Time-dependent normalized fluorescence intensity profiles of xPdots 488, xPdots 561, xPdots 640, and the small-molecule dye Cy5 during continuous laser irradiation. The fluorescence intensities were normalized to their initial values.

As shown in Figures S6–S7, microtubule structures labeled with xPdots remained well defined throughout the entire imaging process under continuous laser irradiation, exhibiting only minor fluorescence decay. In contrast, the fluorescence signal of Cy5-labeled microtubules decreased rapidly over time. Quantitative analysis further revealed that xPdot 488, xPdot 561, and xPdot 640 retained a high proportion of their initial fluorescence intensity during continuous irradiation, whereas Cy5 displayed pronounced photobleaching behavior. These results clearly demonstrate that xPdots exhibit significantly improved photostability compared with the conventional small-molecule dye Cy5.

2.4. Fluorescence lifetime of xPdots compared with conventional Pdots

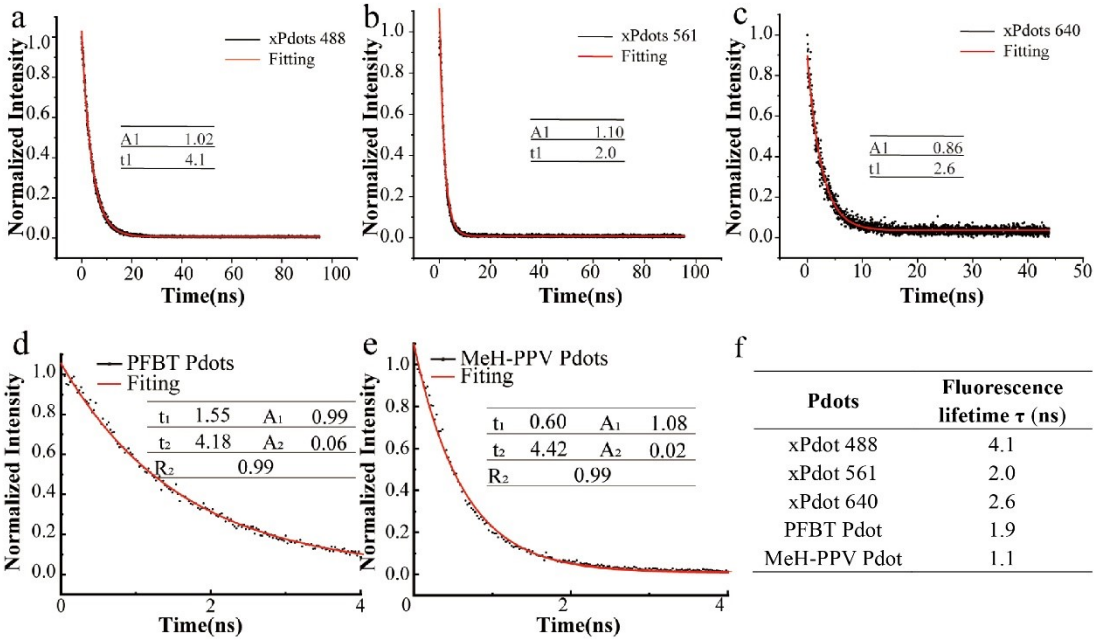

f

Pdots	Fluorescence lifetime τ (ns)
xPdot 488	4.1
xPdot 561	2.0
xPdot 640	2.6
PFBT Pdot	1.9
MeH-PPV Pdot	1.1

Figure S8. Fluorescence lifetime measurement of xPdots and two commercially available Pdots.

As shown in Figure S8, The fluorescence lifetimes of xPdots 488, 561, and 640 were determined to be 4.1 ns, 2.0 ns, and 2.6 ns, respectively. These values are longer than those measured for conventional commercially available Pdots, such as PFBT Pdots (1.9 ns)and MeH-PPV Pdots (1.1 ns). The relatively longer fluorescence lifetimes of xPdots are consistent with their improved depletion behavior under STED conditions and further support their suitability as probes for STED imaging.

2.5. NMR Spectra

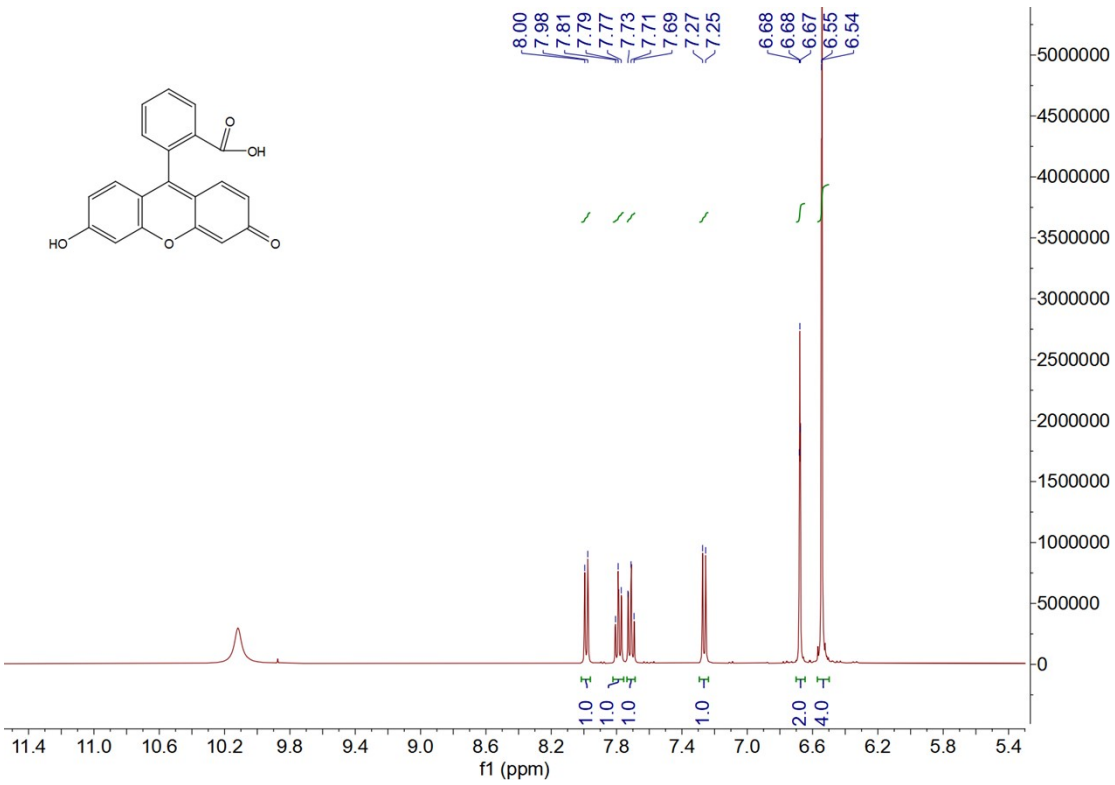

^{1}H NMR Spectra for Xanthene 488

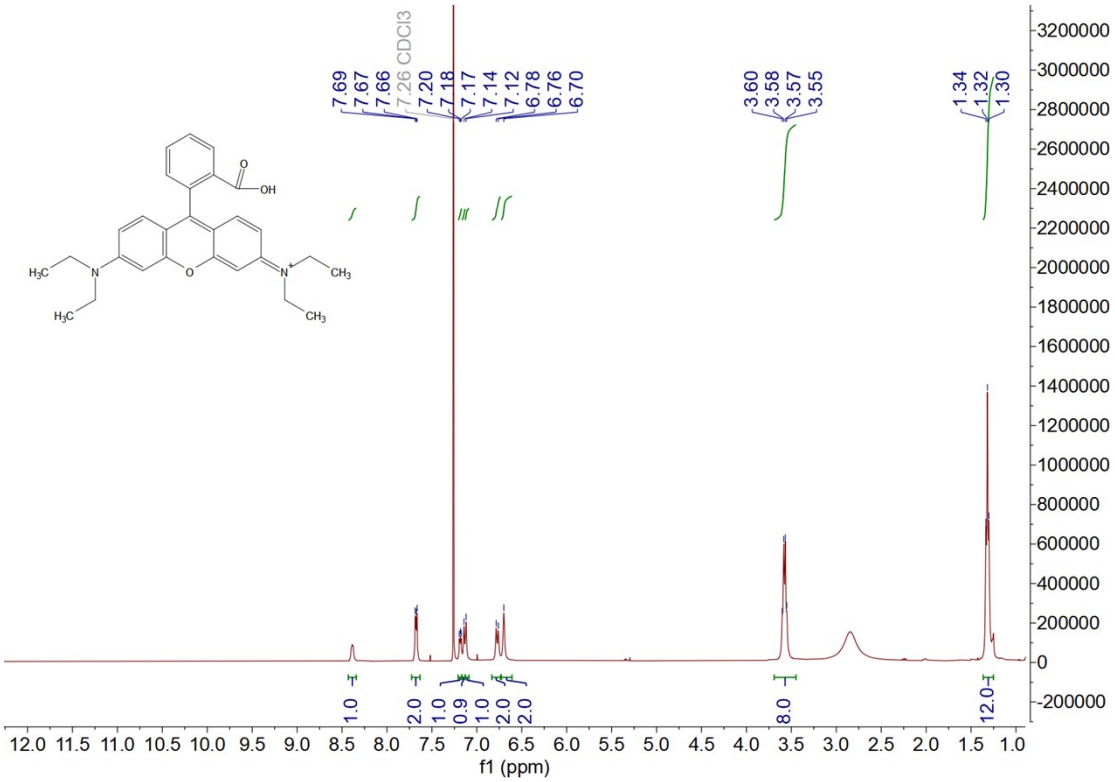

^{1}H NMR Spectra for Xanthene 561

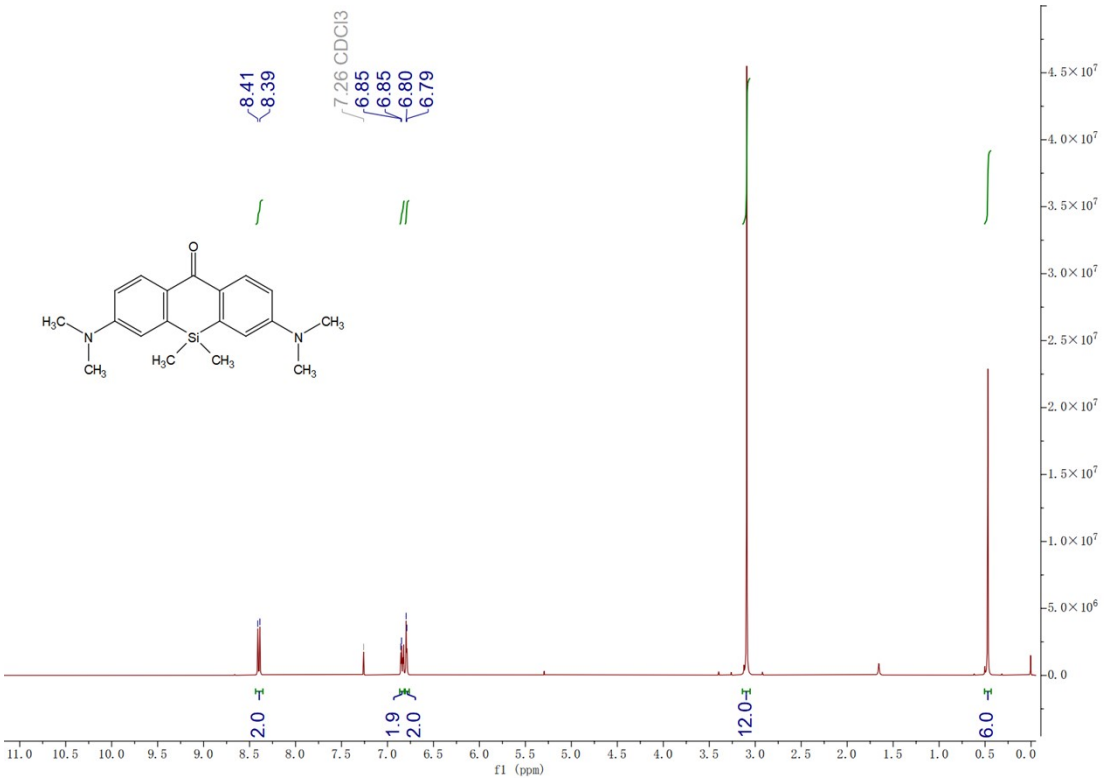

^{1}H NMR Spectra for Xanthene 640 precursor compound